nature astronomy

Article

https://doi.org/10.1038/s41550-023-02191-7

Diverse volcanism and crustal recycling on early Mars

Received: 21 December 2022

Accepted: 22 December 2023

Published online: 12 February 2024

Check for updates

Joseph R. Michalski[1] ✉, A. Deanne Rogers[2], Christopher S. Edwards[3], Aster Cowart[4] & Long Xiao[5]

The relatively well-preserved ancient crust of Mars provides a natural window into early planetary evolution not available on Earth due to sustained tectonic recycling and erosion on this planet. Mars has generally been considered a one-plate basaltic planet, though recent evidence suggests magmatic evolution resulting in felsic crust might have occurred sporadically. Here we show multiple lines of evidence for diverse volcanism and complex volcanotectonics in the southern highlands of Mars within and around the ~3.5–4-billion-year-old Eridania basin. Infrared remote sensing reveals bimodal volcanism consisting of olivine-bearing basalts and voluminous, widespread dacitic (64–69% SiO_2, and possibly higher) volcanic deposits within a region of high crustal potassium. The diverse igneous compositions are associated with an extraordinary number and morphological range of volcanic structures, including domes, stratovolcanoes, calderas and pyroclastic shields occurring proximal to large (hundreds of kilometres in diametre) basins within the Eridania region. The 2–4 km-deep topographically concave-up basins have crustal thicknesses 10–20 km thinner than adjacent terrain and disrupt patterns of deeply seated remnant crustal magnetism. The Eridania basins may represent ancient episodes of crustal recycling via lithospheric delamination in which altered, hydrated volcanic materials were cycled downward and melted resulting in magmatic evolution analogous to pre-plate tectonic processes on the Archaean Earth.

Before the emergence of a recognizable form of plate tectonics on Earth circa 3 billion years ago (Ga), the Earth was resurfaced by earlier forms of volcanotectonics[1]. Despite the importance for understanding planetary evolution and the environments where life originated on this planet, there is little consensus on the style and process of crustal resurfacing in the Eoarchean and Paleoarchean (3.2–4.0 Ga)[2]. Understanding Archaean crustal evolution relies heavily on models and geochemical proxies within rare, highly metamorphosed and metasomatized terranes because most of our planet's ancient crust has been lost to erosion and younger crustal recycling[3].

Geological exploration of other rocky planets provides clues to early crustal evolution and volcanotectonic processes because other bodies exemplify comparable geosystems with variable mass, gravity and composition[4]. Observed through the lenses of different gravity fields, bulk planet compositions and heat flow, it is possible to test models for crustal resurfacing and so discover the steps that led to plate tectonics and other forms of crustal recycling[5]. The planet Mars represents a particularly valuable puzzle piece in this regard. Approximately 70% of the Martian surface is >3 billion years old, and ~45% is older than 3.6 billion years[6]. Though the crust is heavily impact cratered, the

[1]Dept of Earth Sciences & Laboratory for Space Research, University of Hong Kong, Hong Kong, China. [2]Department of Geosciences, Stony Brook University, Stony Brook, NY, USA. [3]Department of Astronomy and Planetary Sciences, Northern Arizona University, Flagstaff, AZ, USA. [4]Planetary Science Institute, Tucson, AZ, USA. [5]China University of Geosciences, Wuhan, China. ✉e-mail: jmichal@hku.hk

https://doi.org/10.1038/s41550-023-02191-7

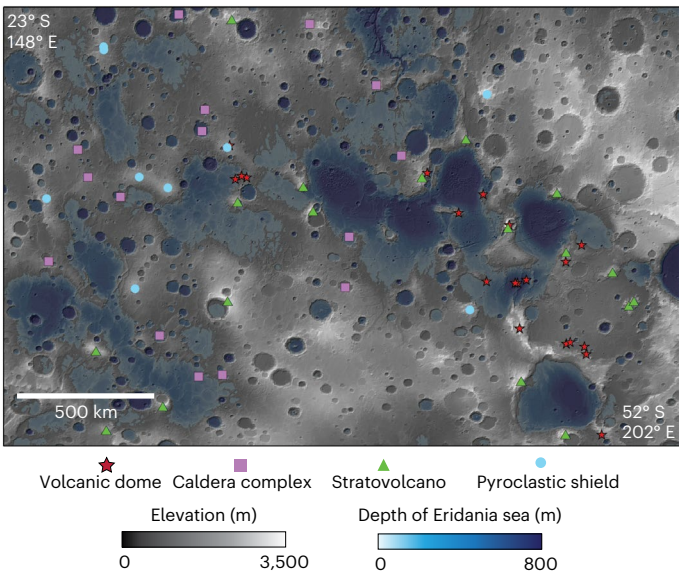

Fig. 1 | A topographic map of the Eridania region of Mars. MOLA/HRSC elevation data are draped onto hillshade data. Blue tones are used to show the extent and depth of a large inland sea. Volcanic structures described in this study are classified by morphology and morphometrics.

ancient geologic record remains largely intact and therefore provides an invaluable window into early solar system geological conditions[7] and clues to early crustal evolution.

One essential element in the pathway toward plate tectonics is the existence of continents composed of felsic rock[8], but it remains unclear how the earliest tronjemite–tonalite–granodiorite (TTG) or granite–monzonite–syenite (GMS) plutons and related dacite–rhyolite volcanic systems formed on Earth[9]. It is possible that plume-dominated volcanism in an Icelandic-type setting resulted in rhyolitic volcanism through fractional crystallization driven by melting of weathered, hydrated volcanic materials buried in a high geothermal gradient[10]. On the Archaean Earth, lithospheric delamination resulted in crustal recycling of altered, hydrated crust[11–14], and a similar process has been hypothesized for ancient Mars[15–17].

Mars has long been considered a basaltic world with little igneous diversity, but discoveries in the past decade of enclaves of evolved plutonic and volcanic rocks[18–24] hint that this paradigm requires reframing. This work explores the geology and volcanology of the Eridania basins and surrounding terrains in Terra Cimmeria and Terra Sirenum (~180° E, 30° S). This region contains the strongest signature of remnant crustal magnetism on the planet[25], a high potassium anomaly[26], large contrasts in crustal thickness[27] and volcanically and structurally complex Hesperian–Noachian (>3 Ga) crust[6,28–31] within a unique Martian terrane or crustal block[32]. In addition, the region contains evidence for an ancient Martian sea approximately three times the size of the modern Caspian Sea on Earth with associated widespread alteration and hydration of the crust[33]. Though this part of Terra Cimmeria and Terra Sirenum is recognized for having some volcanic vents and structures[6,28,31,34,35], the provenance of olivine-rich flood lavas and the widespread (1.8×10^6 km^2), voluminous (~10^6 km^3) 'Electris' suite of airfall deposits[28,36] remains enigmatic[37]. This work describes a diverse suite of volcanic structures and associations of those structures with tectonics and crustal properties. The diverse volcanism is associated with felsic volcanic compositions which are unlike any other suite of recognized deposits or volcanic region on Mars.

Volcanic morphology and morphometrics

The Eridania region of Mars contains at least 63 (identified here) and possibly hundreds of volcanoes, many of which were previously unrecognized (Fig. 1, Supplementary Table 1 and Supplementary Fig. 1). We classified the structures into four categories based on their morphologies and morphometric characteristics: (1) volcanic domes, (2) stratovolcanoes, (3) pyroclastic shields and (4) caldera complexes (Fig. 2). Volcanic domes are characterized by their smaller size (average diameter, d = 14 km), low height (average height, h = 0.8 km), viscous flow features, lobate plan view, sharp edges or escarpments (Supplementary Fig. 1) and high average height/diameter ratio (h/d) of 0.056 (Fig. 3). Stratovolcanoes have some similar features to domes, such as steep escarpments and some lobate flow features elevated on the structure, but overall have a shallow, conical morphology and often contain summit or flank craters, sometimes structurally linked through faults and fractures. They are typically 40–80 km in diameter and are the tallest of the structures described here, with heights reaching 2–3 km above the surrounding terrain with moderate h/d (0.036) (Fig. 3). Pyroclastic shields are large features approximately 100 km in diameter with low heights (~1.1 km) and low corresponding h/d (.011). They are quasi-circular in plan view and contain a summit or near-summit crater. A striking and important characteristic of the pyroclastic shields and stratovolcanoes is that they contain dense valley networks eroded into their flanks (Extended Data Fig. 1), which we propose is a reflection of the susceptibility to erosion of their pyroclastic rock. Caldera complexes are unique because they are destructional volcanic features, not constructional ones[38], hence their negative average h/d value (−0.015). They form through explosive volcanism and surface collapse but build no central edifice. A critical aspect of their morphologies is the occurrence of multiple structurally linked topographic depressions lacking the characteristic features of impact craters such as raised rims, ejecta and central peaks[38]. Some of the plains-style caldera complexes in the Terra Cimmeria and Terra Sirenum terrains have as many as 14 structurally linked depressions.

Morphometrics illustrate important trends regarding Martian volcanology and also shine a light on critical differences between volcanism on the Earth and Mars. The smallest features described here are volcanic domes, and the largest-diameter features are shield volcanoes; stratovolcanoes have similar heights to shields but with higher h/d (Fig. 3). The Martian volcanic structures discovered here follow the same trend as comparable classes of volcanoes on Earth, but they are shifted towards larger diameters, and therefore the Martian features have lower h/d values (Fig. 3). This can be explained in the context of Mars's lower-gravity environment (38% of Earth), resulting not only in more explosive volcanism but dispersal of pyroclasts further from the vents, resulting in lower profile features[39]. One key difference on Mars is the occurrence of very large shield volcanoes, comparable in diameter to those on the Moon, but much taller. Those features formed largely through sustained hot-spot volcanism over billions of years, into the Amazonian (<3 Ga) (ref. 40). The older, smaller, more subtle volcanic features described here could be present throughout the ancient crust of Mars[41] and could provide a fundamental connection between source and sink for many highland deposits currently lacking provenance[42].

Composition of volcanic materials

Thermal infrared remote sensing of the Eridania region demonstrates a diversity of compositions among the volcanic materials. Decorrelation-stretched Thermal Emission Imaging System (THEMIS) images (Fig. 4 and Supplementary Fig. 2) show mafic to ultramafic surfaces as purple-blue and more felsic surfaces as yellow[24] (Fig. 4a), linking qualitative compositional variation to morphological context[43] (Extended Data Fig. 2). Surface composition is quantitatively constrained by fitting a spline curve to the atmospherically corrected surface emissivity spectra (Fig. 4b), providing a central wavelength of the Si–O stretching absorption in silicates[44], which is correlated with SiO_2 per cent (Fig. 4c). THEMIS spline fits suggest that the felsic volcaniclastic surfaces and volcanic domes have relatively high silica content (Fig. 4b,c and Supplementary Fig. 4). By comparing the THEMIS

https://doi.org/10.1038/s41550-023-02191-7

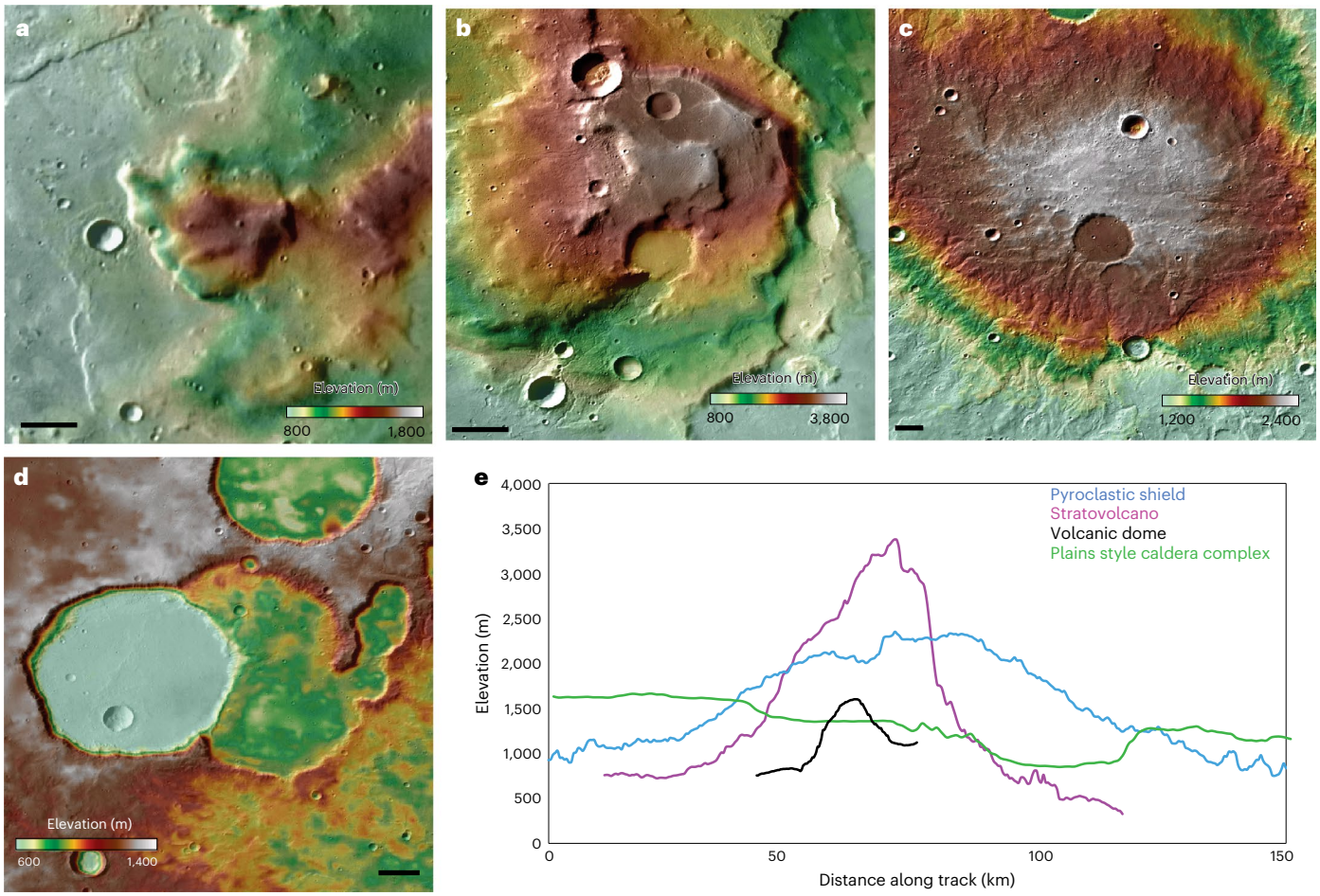

Fig. 2 | Morphology of four classes of volcanoes in the Eridania region. a,**b**,**c**,**d**, Type examples of a volcanic dome (**a**), stratovolcano (**b**), pyroclastic shield (**c**) and caldera complex (**d**) are shown with MOLA/HRSC elevation data draped over Mars Context Imager data. **e**, Topographic profiles of each feature represent SW–NE profile lines at each site. Scale bars, 5 km.

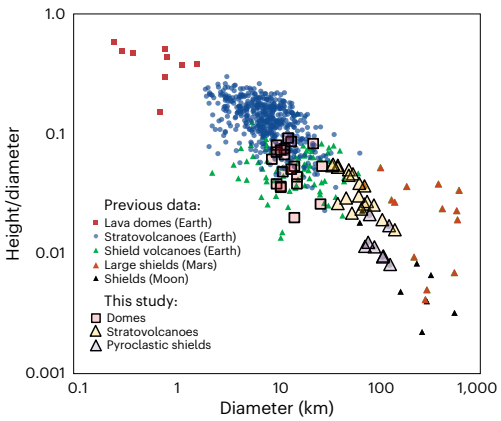

Fig. 3 | Morphometric data for volcanic structures. Data for volcanic domes, stratovolcanoes and pyroclastic shields in the Eridania region described in this study are compared to similar measurements for structures on the Earth, Moon and Mars. Diameter and height/diameter ratios are shown for rhyolitic–dacitic domes, stratovolcanoes and shield volcanoes on Earth, large shields on Mars and large shields on the Moon.

spline fits to those of rocks measured in the laboratory and adjusted to similar spectral sampling, it is possible to quantitatively constrain the SiO_2 content of the Martian volcanic materials. If the Martian rocks are alkaline volcanics, they are likely 64–69% SiO_2 and if they are glass-rich, they could be 71–75% SiO_2. Given their high potassium content and morphology, it is unlikely they are glass-poor subalkaline rocks, but if they are in this category, the silica content is estimated at 58–59% SiO_2 (Fig. 4c). It bears noting that basaltic sand on the felsic surfaces could make the silica content appear lower than it is in the primary rock. High silica content in the same surfaces is supported by high values of the Thermal Emission Spectrometer (TES) silica index, which independently measures Si–O bending absorptions in the region (Extended Data Fig. 3). TES and THEMIS data both suggest little or no quartz and high feldspar/pyroxene ratios. The high-silica volcanic deposits generally correspond to light-toned, buff-coloured, layered or massively bedded, surface draping material in high-resolution images (Fig. 4d,e), but THEMIS data of some central uplifts of impact craters shows that silica-rich material exists to at least 5 km depth (Supplementary Fig. 2).

Near-infrared reflectance spectra from the Compact Reconnaissance Imaging Spectrometer for Mars (CRISM) of subaerially deposited volcanic deposits are generally spectrally unremarkable, with the exception of their evidence for bound water that could occur as zeolites or clay minerals (Supplementary Fig. 3) formed through chemical weathering. By contrast, CRISM spectra of ancient volcanic deposits in the deep basin below interpreted sea level contain abundant and diverse Fe- and Mg-rich clay minerals, carbonates, and other alteration phases[33]. Mafic volcanics deposited subaerially occur as flood lavas and show strong absorptions related to olivine and pyroxene. CRISM is sensitive to some hydrous igneous minerals such as mica and amphibole, but neither is detected.

https://doi.org/10.1038/s41550-023-02191-7

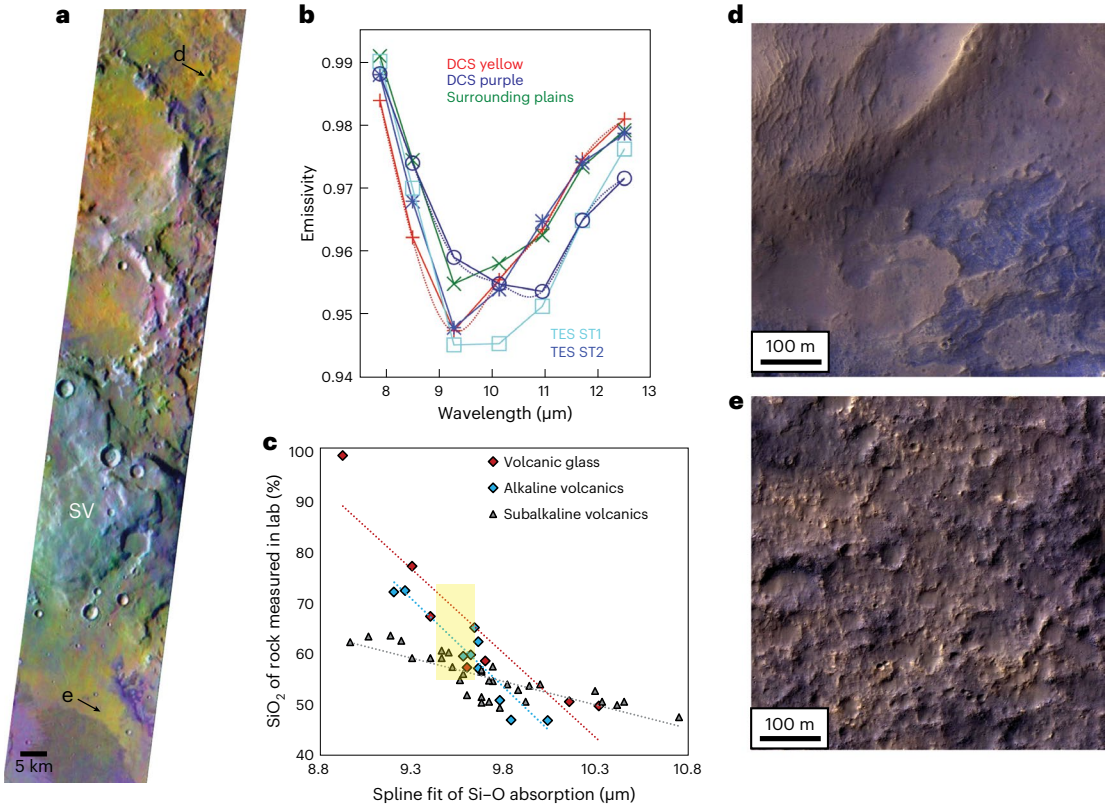

Fig. 4 | Infrared and image data showing felsic volcanic materials in the Eridania region. a, A THEMIS decorrelation-stretched image (I08708002) shows felsic materials as yellow and mafic material as purple surrounding a stratovolcano (labelled 'SV') at 170.3° E, 35° S. **b**,**c**, Surface emissivity spectra of the felsic (yellow) and mafic (purple) surfaces are compared to global average TES surface type 1 (ST1) and surface type 2 (ST2). Spline fits to the THEMIS data shown in **b** correspond to 9.36–9.5 μm for the yellow felsic surfaces and 10.74 μm for the purple mafic, and when compared to the plot shown in **c** of the spline fits for laboratory rocks and glasses, these values suggest high-silica compositions (yellow zone in **c**) as described in the main text. **d**,**e**, HiRISE data show that the felsic material is buff- to pink-coloured massive (**d**) to finely layered surface deposits (**e**), which we interpret as volcanic ash (images ESP_025301_1440 and ESP_023745_1465, respectively). Locations of HiRISE infrared-red-blue/green images are indicated with arrows in **a**.

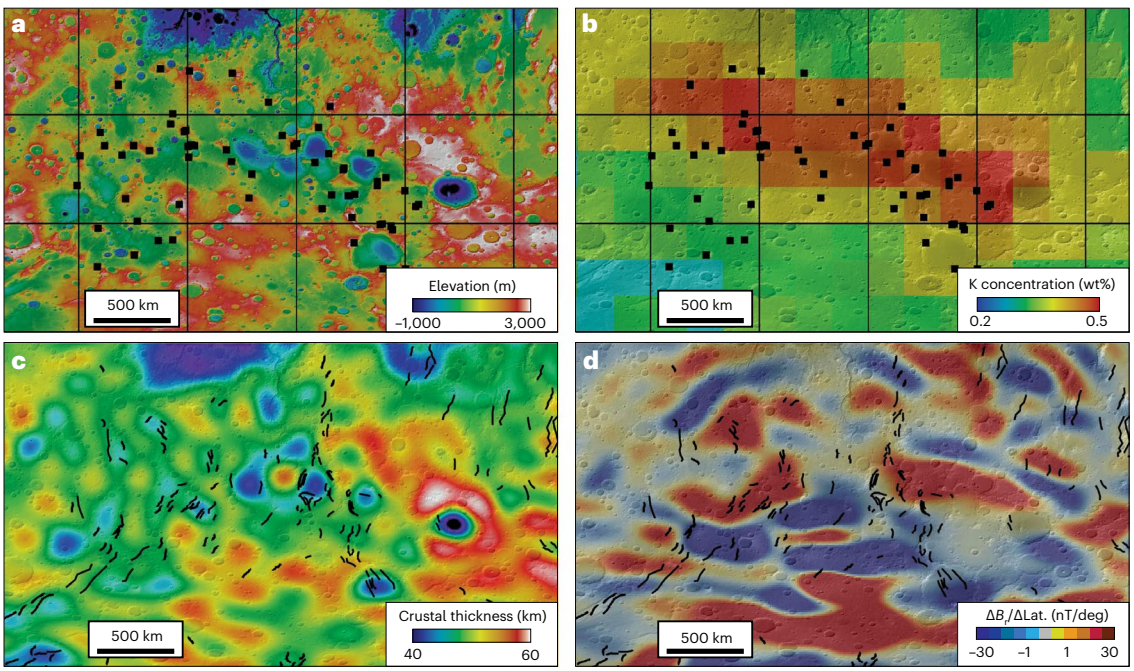

Fig. 5 | Volcanic structures in the context of regional crustal properties. **a**, MOLA elevation data show that the Eridania basin is composed of a series of 1- to 3-km-deep subbasins. Volcanoes identified in this study are marked with black squares. **b**, The volcanoes occur in a zone of high crustal potassium. **c**,**d**, The basins (**c**) have 10 to 20 km thinner crusts. Wrinkle ridges marked by black lines (**c**,**d**) occur in NE- and NW-trending lineaments, which also mark zones (**d**) of disruption of the remnant crustal magnetism. Lat., latitude; B_r, radial magnetic component.

https://doi.org/10.1038/s41550-023-02191-7

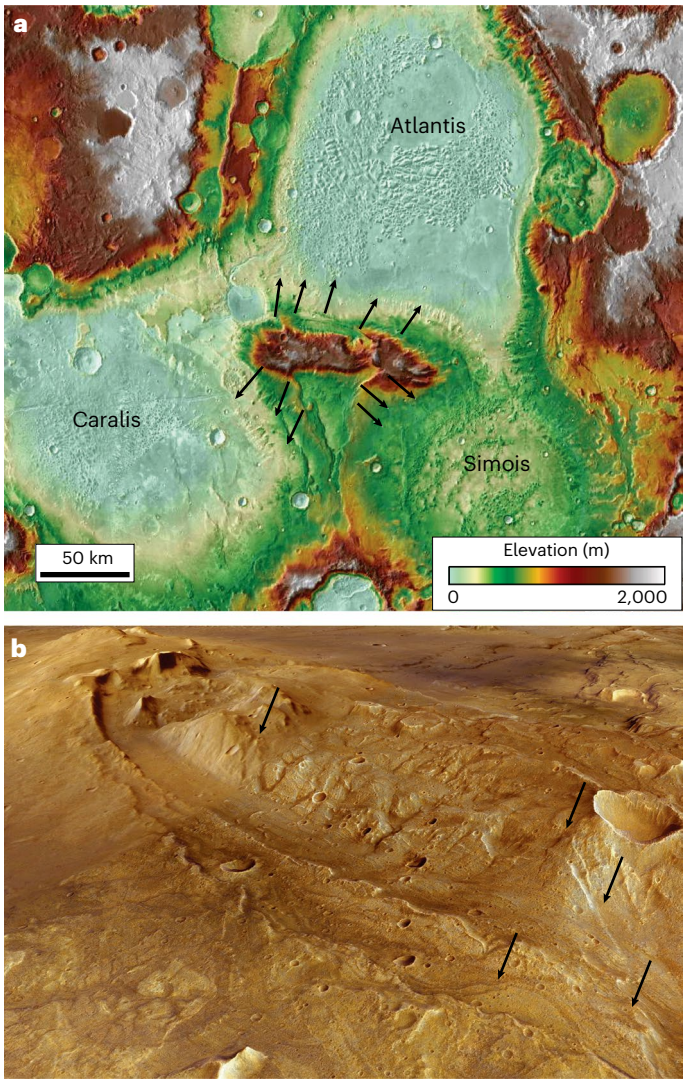

Fig. 6 | Folded rocks in a diapir-like structure. a, MOLA/HRSC elevation data draped onto THEMIS daytime infrared data illustrate that three subbasins (Atlantis, Caralis and Simois) are separated only by a large antiformal structure. Black arrows indicate dip direction of layers. **b**, An HRSC colour image draped over topography shows steeply dipping layers in the north flank of the antiform. Perspective is looking SE from the north side of the structure. Arrows point to the traces of steeply dipping layers.

Volcanotectonics and crustal recycling

The morphologically and compositionally diverse volcanism observed in Terra Cimmeria and Terra Sirenum points to an episode of magmatic evolution and possible crustal recycling. The volcanoes occur within a zone of potassium-enrichment (Fig. 5a), but the footprint of the Gamma Ray Spectrometer (GRS) data is large (~500 km) and it is not possible to trace the K to host rocks from those data. While it would be useful to know the sodium abundance in the region, GRS is not able to measure this element. The K likely occurs within feldspars and volcanic glass, both of which appear relatively abundant in the area from TES and THEMIS data.

The volcanic structures occur within and adjacent to the Eridania basin, which is composed of a WNW-trending suite of five or more large (~200 km diameter), deep (1–3 km) subbasins[45] (Fig. 5b). It is likely that volcanism occurred throughout the basins, but the morphologies of the volcanic vents are very different in the basin floor because they occurred beneath ~400–1,200 m of water in the Eridania sea, resulting in 20–50 bars of pressure[33]. The range of volcanic styles observed proximal to the basins occurred because these volcanoes erupted subaerially (Extended Data Fig. 1).

Based on gravity measurements, the crustal thickness in the basins is 10–20 km thinner than in the immediately adjacent highlands (Fig. 5c). Strong E–W-trending remnant magnetic stripes thought to originate from magmatic intrusions at depths of tens of kilometres[46,47] are disrupted in the terrain where the basins occur (Fig. 5d), suggesting a connection between deep subsurface processes and surface expression. Though the basins could have an impact origin, they are unlike Martian impact basins because they have much lower circularity (average of 0.83) compared to Martian impact craters such as Gusev Crater, Jezero Crater, Gale Crater or Isidis basin (average of 0.98; Supplementary Fig. 5.); they have concave-up floors rather than flat floors and lack any typical features of impact such as raised rims, ejecta, terraced walls or central peaks.

The margins of the irregularly or rhombohedrally shaped basins are generally defined by structures including large escarpments and wrinkle ridges or thrust faults (Fig. 5c; Extended Data Fig. 4)[6,29], The amount of offset of the thrusts can be difficult to determine, but minimum values reach up to 15 km calculated where circular impact or volcanic craters have been overthrust by the hanging wall (Extended Data Fig. 5). Strikingly, three large subbasins, Atlantis Chaos, Caralis Chaos and Simois Colles, are separated only by the presence of a ~140-km-long WNW-trending fold complex (Fig. 6). The antiformal structure bears some characteristics of a diapir or salt dome, but no salts are detected in the THEMIS data. A three-dimensional perspective (Fig. 6b) shows steeply dipping layers flanking the structure. High-resolution images of the small impact craters on fold axes show that surface exposures of layering are not deflected by topography, indicating that the layers have near vertical dips (Extended Data Fig. 6).

The suite of volcanic, structural, geochemical, geophysical and topographic observations within and around the Eridania basins can be understood in the context of vertical tectonics. Before plate tectonics took hold on the Archaean Earth circa 2.5 billion years ago, crustal evolution on this planet was governed in part by vertical tectonics driven by eclogitization and delamination of the lithosphere[12,13]. Observational tests for convective overturn of the crust due to gravitational instabilities from Archaean terranes include eruption of thick volcanic deposits, crustal downwarping and the formation of basin-marginal diapiric-like folds[13]. The incorporation of hydrated, hydrothermally altered and chemically weathered volcanics into the deep crust and upper mantle via catastrophic, episodic overturn through vertical tectonics was likely an important step in evolution of felsic rocks and ultimately continental material on Earth[11,12], and a similar process might have operated on early Mars, as evidenced in the Eridania region. The observation of evolved igneous rocks, structurally defined basins and folded volcanic rocks and sediments in diapiric structures are all consistent with a model of vertical recycling of the ancient crust of Mars.

The wide range of volcanic styles evident in the Eridania region suggests that similar structures, including domes, stratovolcanoes, small pyroclastic shields and calderas[38], could be much more widespread in the ancient Martian crust than is currently recognized[41]. Evidence for diverse volcanic compositions in highland terranes also challenges the long-held paradigm that Mars is purely a basaltic world and without crustal recycling. Further, Eridania contains a wide range of likely subaqueous and coastal volcanoes analogous to the hypothesized geology of the Eoarchean or Mesoarchean Earth. The chemically and physically diverse settings present in this region of Mars provide a close analogue to both seafloor and land-based hydrothermal origin of life scenarios proposed for the Earth[48,49].

Methods

Morphometric analyses

Volcanic features were identified using THEMIS daytime infrared data and Mars Context Imager images, including the global mosaic created

by the Murray Lab. Where available, High Resolution Imaging Science Experiment (HiRISE) visible images were also used to describe and interpret volcanic morphologies. Visible and infrared images were combined with elevation data obtained at 200 metres per pixel resolution from the Mars Orbiter Laser Altimeter (MOLA) and the High Resolution Stereo Camera (HRSC). Elevation and slope data were instrumental in the identification of new features and essential for quantifying diameter and height characteristics.

Compositional mapping

The wavelength of the emissivity minimum between ~8 and 12 μm corresponding to Si–O stretching was used to estimate silica content. To more precisely estimate the wavelength position of the surface emissivity minimum in multispectral data, we calculated a cubic spline interpolation to atmospherically corrected THEMIS emissivity spectra (bands 3–9). The wavelength position of the spline-fit minimum was then mapped on a pixel-by-pixel basis. We also applied cubic spline fits to laboratory thermal emission spectra (degraded using THEMIS filter response functions) from felsic, anorthositic, mafic and ultramafic rocks (Supplementary Information). Additional spline-fit minimum values were calculated for a suite of volcanic rocks, ranging from basalts to dacites.

Data availability

All data used in this study are available in the public domain and accessible through the JMARS online software platform (https://jmars.asu.edu/).

References

1. O'Neill, C., Turner, S. & Rushmer, T. The inception of plate tectonics: a record of failure. *Philos. Trans. R. Soc. A* **376**, 20170414 (2018).
2. Windley, B. F., Kusky, T. & Polat, A. Onset of plate tectonics by the Eoarchean. *Precambrian Res.* **352**, 105980 (2021).
3. Brown, M., Johnson, T. & Gardiner, N. J. Plate tectonics and the Archean Earth. *Annu. Rev. Earth Planet. Sci.* **48**, 291–320 (2020).
4. van Thienen, P., Vlaar, N. J. & van den Berg, A. P. Plate tectonics on the terrestrial planets. *Phys. Earth Planet. Inter.* **142**, 61–74 (2004).
5. Palin, R. M. et al. Secular change and the onset of plate tectonics on Earth. *Earth-Sci. Rev.* **207**, 103172 (2020).
6. Tanaka, K. L. et al. Geologic map of Mars. *U.S. Geological Survey* http://pubs.usgs.gov/sim/3292/ (2014).
7. Michalski, J. R. et al. The Martian subsurface as a potential window into the origin of life. *Nat. Geosci.* **11**, 21–26 (2018).
8. Hawkesworth, C. J. & Kemp, A. I. S. Evolution of the continental crust. *Nature* **443**, 811–817 (2006).
9. Condie, K. C. in *Evolution of Archean Crust and Early Life*, Vol 7. (eds Dilek, Y. & Furnes H.) 179–193 (Springer, 2014); https://doi.org/10.1007/978-94-007-7615-9_7
10. Reimink, J. R., Chacko, T., Stern, R. A. & Heaman, L. M. Earth's earliest evolved crust generated in an Iceland-like setting. *Nat. Geosci.* **7**, 529–533 (2014).
11. Fischer, R. & Gerya, T. Early Earth plume-lid tectonics: a high-resolution 3D numerical modelling approach. *J. Geodyn.* **100**, 198–214 (2016).
12. Johnson, T. E., Brown, M., Kaus, B. J. P. & VanTongeren, J. A. Delamination and recycling of Archaean crust caused by gravitational instabilities. *Nat. Geosci.* **7**, 47–52 (2014).
13. Van Kranendonk, M. J., Collins, W. J., Hickman, A. & Pawley, M. J. Critical tests of vertical vs. horizontal tectonic models for the Archaean East Pilbara Granite–Greenstone Terrane, Pilbara Craton, Western Australia. *Precambrian Res.* **131**, 173–211 (2004).
14. Collins, W. J., Van Kranendonk, M. J. & Teyssier, C. Partial convective overturn of Archaean crust in the east Pilbara Craton, Western Australia: driving mechanisms and tectonic implications. *J. Struct. Geol.* **20**, 1405–1424 (1998).
15. Papike, J. J., Burger, P. V., Shearer, C. K. & McCubbin, F. M. Experimental and crystal chemical study of the basalt–eclogite transition in Mars and implications for Martian magmatism. *Geochim. Cosmochim. Acta* **104**, 358–376 (2013).
16. Semprich, J. & Filiberto, J. High-pressure metamorphic mineralogy of the Martian crust with implications for density and seismic profiles. *Meteorit. Planet. Sci.* **55**, 1600–1614 (2020).
17. Zhou, W.-Y. et al. High pressure-temperature phase equilibrium studies on Martian basalts: Implications for the failure of plate tectonics on Mars. *Earth Planet. Sci. Lett.* **594**, 117751 (2022).
18. Payré, V., Salvatore, M. R. & Edwards, C. S. An evolved early crust exposed on Mars revealed through spectroscopy. *Geophys. Res. Lett.* **49**, e2022GL099639 (2022).
19. Sautter, V. et al. In situ evidence for continental crust on early Mars. *Nat. Geosci.* https://doi.org/10.1038/ngeo2474 (2015).
20. Wray, J. J. et al. Prolonged magmatic activity on Mars inferred from the detection of felsic rocks. *Nat. Geosci.* https://doi.org/10.1038/ngeo1994 (2013).
21. Carter, J. & Poulet, F. Ancient plutonic processes on Mars inferred from the detection of possible anorthositic terrains. *Nat. Geosci.* **6**, 1008–1012 (2013).
22. Bandfield, J. L., Hamilton, V. E., Christensen, P. R. & McSween, H. Y. Identification of quartzofeldspathic materials on Mars. *J. Geophys. Res.* **109**, E10009 (2004).
23. Christensen, P. R. et al. Evidence for magmatic evolution and diversity on Mars from infrared observations. *Nature* **436**, 504–509 (2005).
24. Bandfield, J. L. Extended surface exposures of granitoid compositions in Syrtis Major, Mars. *Geophys. Res. Lett.* **33**, L06203 (2006).
25. Connerney, J. E. P. et al. Tectonic implications of Mars crustal magnetism. *Proc. Natl Acad. Sci. USA* **102**, 14970–14975 (2005).
26. Boynton, W. V. et al. Concentration of H, Si, Cl, K, Fe, and Th in the low- and mid-latitude regions of Mars. *J. Geophys. Res. Planets* **112**, E12S99, https://doi.org/10.1029/2007JE002887 (2007).
27. Goossens, S. et al. Evidence for a low bulk crustal density for Mars from gravity and topography. *Geophys. Res. Lett.* **44**, 7686–7694 (2017).
28. Brož, P., Bernhardt, H., Conway, S. J. & Parekh, R. An overview of explosive volcanism on Mars. *J. Volcanol. Geotherm. Res.* **409**, 107125 (2021).
29. Molina, A., de Pablo, M. Á., Hauber, E., Le Deit, L. & Fernández-Remolar, D. (Carlos). Geology of the Ariadnes Basin, NE Eridania quadrangle, Mars – 1:1Million. *J. Maps* **10**, 487–499 (2014).
30. Wilson, L. & Head, J. W. Tharsis-radial graben systems as the surface manifestation of plume-related dike intrusion complexes: Models and implications. *J. Geophys. Res.* **107**, 1-1–1-24 (2002).
31. Brož, P., Hauber, E., Platz, T. & Balme, M. Evidence for Amazonian highly viscous lavas in the southern highlands on Mars. *Earth Planet. Sci. Lett.* **415**, 200–212 (2015).
32. Bouley, S. et al. A thick crustal block revealed by reconstructions of early Mars highlands. *Nat. Geosci.* **13**, 105–109 (2020).
33. Michalski, J. R., Dobrea, E. Z. N., Niles, P. B. & Cuadros, J. Ancient hydrothermal seafloor deposits in Eridania basin on Mars. *Nat. Commun.* **8**, 15978 (2017).
34. Xiao, L. et al. Ancient volcanism and its implication for thermal evolution of Mars. *Earth Planet. Sci. Lett.* **323–324**, 9–18 (2012).
35. Scott, E. D., Wilson, L. & Head, J. W. H. III Emplacement of giant radial dikes in the northern Tharsis region of Mars. *J. Geophys. Res.* **107**, 3-1–3-10 (2002).
36. Grant, J. A. et al. HiRISE views enigmatic deposits in the Sirenum Fossae region of Mars. *Icarus* **205**, 53–63 (2010).
37. Kerber, L., Head, J. W., Madeleine, J. B., Forget, F. & Wilson, L. The dispersal of pyroclasts from ancient explosive volcanoes on Mars: implications for the friable layered deposits. *Icarus* **219**, 358–381 (2012).

38. Michalski, J. R. & Bleacher, J. E. Supervolcanoes within an ancient volcanic province in Arabia Terra, Mars. *Nature* **502**, 47–52 (2013).
39. Wilson, L. Volcanism in the solar system. *Nat. Geosci*. https://doi.org/10.1038/ngeo529 (2009).
40. Greeley, R. & Spudis, P. Volcanism on Mars. *Rev. Geophys.* **19**, 13–41 (1981).
41. Xiao, L. et al. Ancient volcanism and its implications for thermal evolution of Mars. *Earth Planet. Sci. Lett.* **323–324**, 9–18 (2012).
42. Bandfield, J. L., Edwards, C. S., Montgomery, D. R. & Brand, B. D. The dual nature of the Martian crust: Young lavas and old clastic materials. *Icarus* **222**, 188–199 (2013).
43. Cowart, J. C., Rogers, A. D. & Edwards, C. S. Mapping and characterization of Martian intercrater bedrock plains: insights into resurfacing processes in the Martian cratered highlands. *J. Geophys. Res. Planets* **124**, 3181–3204 (2019).
44. Rogers, A. D. & Nekvasil, H. Feldspathic rocks on Mars: compositional constraints from infrared spectroscopy and possible formation mechanisms. *Geophys. Res. Lett.* https://doi.org/10.1002/2015GL063501 (2015).
45. Irwin, R. P., Howard, A. D. & Maxwell, T. A. Geomorphology of Ma'adim Vallis, Mars, and associated paleolake basins. *J. Geophys. Res.* **109**, E12009 (2004).
46. Connerney, J. E. Magnetic lineations in the ancient crust of Mars. *Sci.* **284**, 794–798 (1999).
47. Nimmo, F. Dike intrusion as a possible cause of linear Martian magnetic anomalies. *Geology* **28**, 391–394 (2000).
48. Damer, B. & Deamer, D. The hot spring hypothesis for an origin of life. *Astrobiology* **20**, 429–452 (2020).
49. Russell, M. J. et al. The drive to life on wet and icy worlds. *Astrobiology* **14**, 308–343 (2014).

Acknowledgements

We acknowledge A. Webb (HKU) and M. Van Kranendonk (UNSW) for insightful conversations that helped shape some of the ideas in this paper. This work was funded by the Hong Kong Research Grants Council Collaborative Research Fund (C7004-21GF) awarded to J.R.M., as well as the Canadian Institute for Advanced Research Earth 4D programme. L.X. was funded by the National Science Fundation of China (42241111).

Author contributions

J.R.M. conceptualized the study, carried out the morphometric analyses and mapping, and wrote the paper. A.D.R. carried out the compositional analyses and edited the paper. C.S.E. contributed spectral imaging and edited the paper. A.C. edited the paper. L.X. edited the paper.

Competing interests

The authors declare no competing interests.

Additional information

Extended data is available for this paper at https://doi.org/10.1038/s41550-023-02191-7.

Supplementary information The online version contains supplementary material available at https://doi.org/10.1038/s41550-023-02191-7.

Correspondence and requests for materials should be addressed to Joseph R. Michalski.

Peer review information *Nature Astronomy* thanks William Rapin and Hannes Bernhardt for their contribution to the peer review of this work.

Reprints and permissions information is available at www.nature.com/reprints.

Publisher's note Springer Nature remains neutral with regard to jurisdictional claims in published maps and institutional affiliations.

Open Access This article is licensed under a Creative Commons Attribution 4.0 International License, which permits use, sharing, adaptation, distribution and reproduction in any medium or format, as long as you give appropriate credit to the original author(s) and the source, provide a link to the Creative Commons license, and indicate if changes were made. The images or other third party material in this article are included in the article's Creative Commons license, unless indicated otherwise in a credit line to the material. If material is not included in the article's Creative Commons license and your intended use is not permitted by statutory regulation or exceeds the permitted use, you will need to obtain permission directly from the copyright holder. To view a copy of this license, visit http://creativecommons.org/licenses/by/4.0/.

© The Author(s) 2024

https://doi.org/10.1038/s41550-023-02191-7

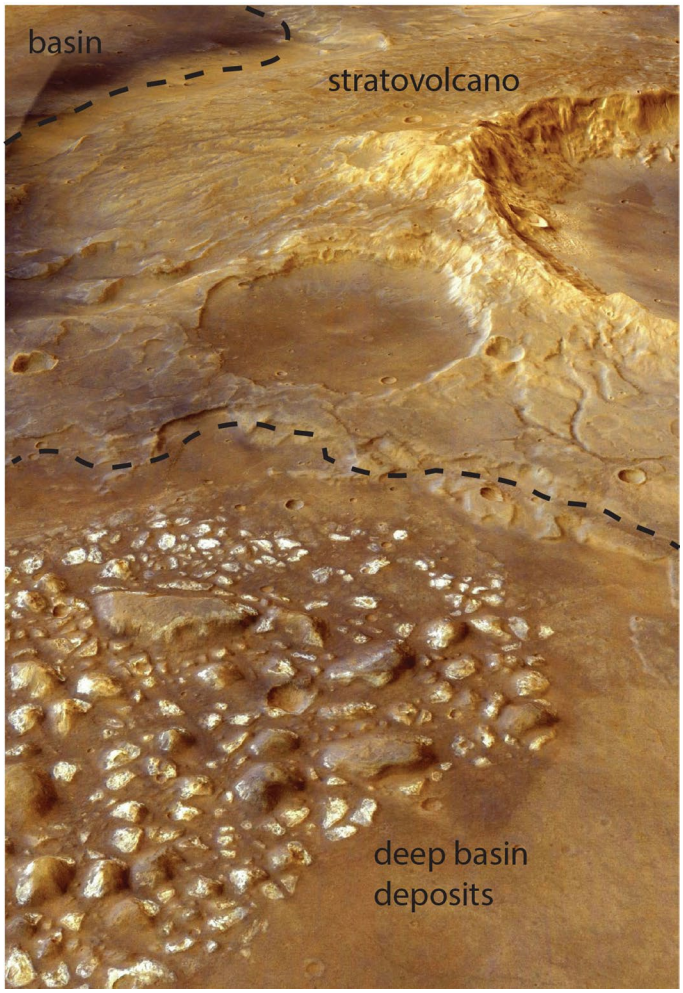

Extended Data Fig. 1 | A 3-D view of a stratovolcano eroded by valley networks. HRSC visible data are draped over digital elevation showing a perspective view of a stratovolcano located at 165 E, 35.9 S. View is looking toward the north. The stratovolcano contains numerous valley networks on its flanks, A steep escarpment occurring at the edge of volcano corresponds with the approximate water level of the proposed Eridania sea. Deep basin deposits containing clay minerals likely formed in a subaqueous environment.

https://doi.org/10.1038/s41550-023-02191-7

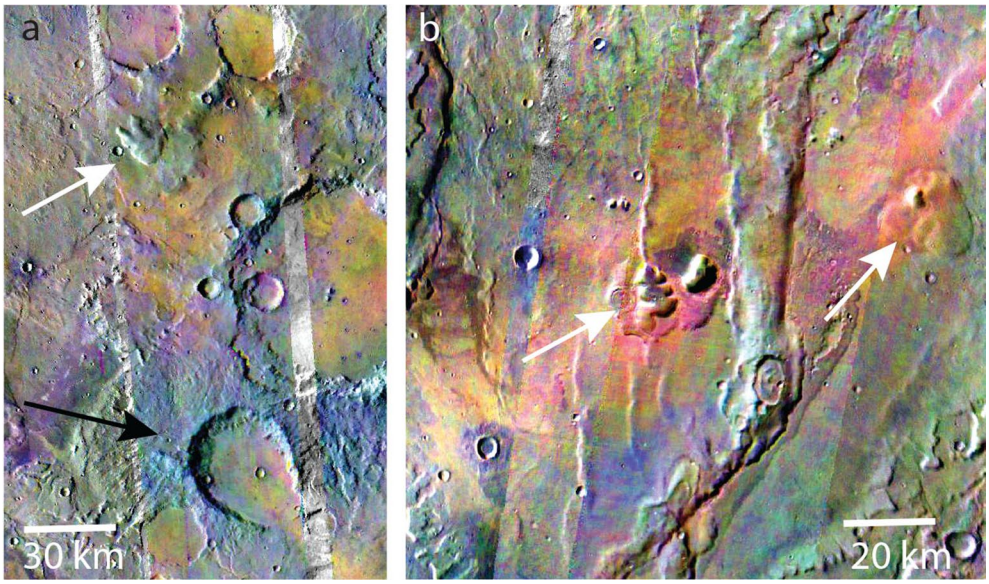

Extended Data Fig. 2 | Association of volcanic domes with felsic surface compositions. THEMIS 8-7-5 decorrelation stretch data show felsic materials for two regions (**a**,**b**) in red and yellow, intermediate compositions in light blue and mafic compositions in purple.

https://doi.org/10.1038/s41550-023-02191-7

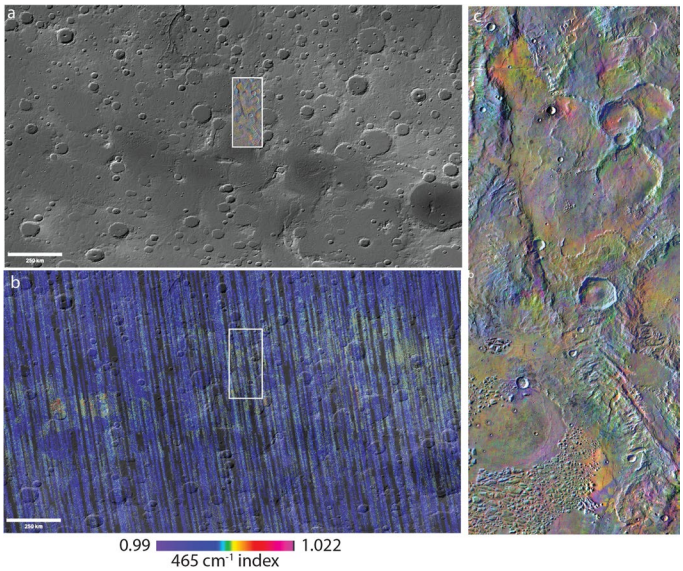

Extended Data Fig. 3 | Occurrence of high-silica materials in the Eridania region. MOLA/HRSC hillshade data are shown in 'a.' The TES 465 cm^{-1} silica index developed by Ruff and Christensen (2007) (b) shows high silica areas in warm colours. A THEMIS DCS mosaic (c) shows felsic materials in yellow colours.

https://doi.org/10.1038/s41550-023-02191-7

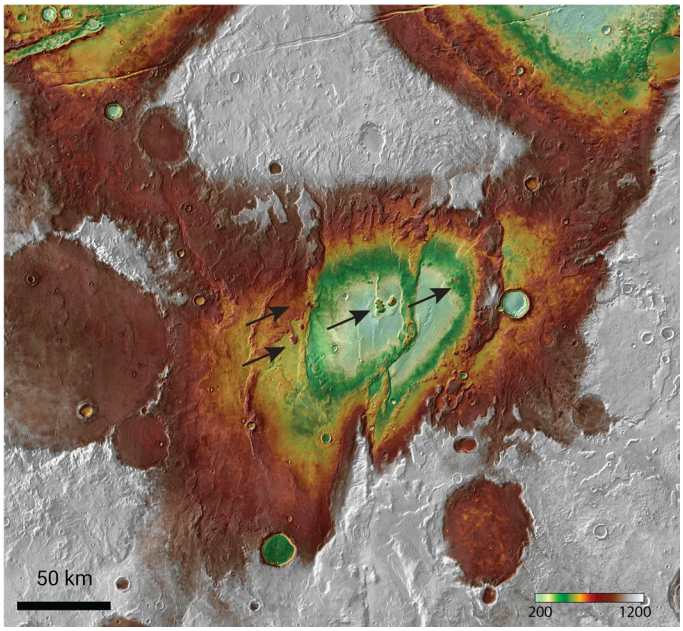

Extended Data Fig. 4 | Occurrence of volcanic structures within a collapse basin. HRSC/MOLA elevation data draped over THEMIS daytime infrared data illustrate the rhombohedral shape and structural complexity of unnamed sub-basins within Eridania. Locations of volcanic domes are indicated by black arrows.

https://doi.org/10.1038/s41550-023-02191-7

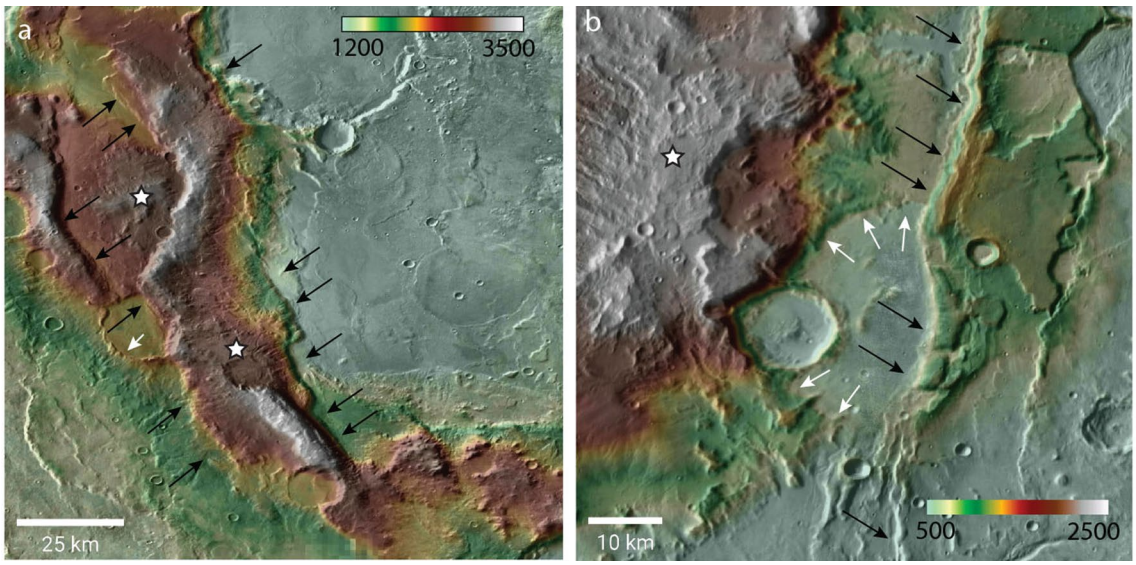

Extended Data Fig. 5 | Structurally complex terrain at basin margins. MOLA/HRSC elevation data are draped over THEMIS daytime infrared data showing NW striking (a) and NNE-striking (b) thrust faults (black arrows). The traces of impact or volcanic craters (white arrows) provide measure of minimum offset, assuming initial circular shapes, of ~7 km in 'a' and 15 km in 'b.' Volcanic structures are marked by stars.

https://doi.org/10.1038/s41550-023-02191-7

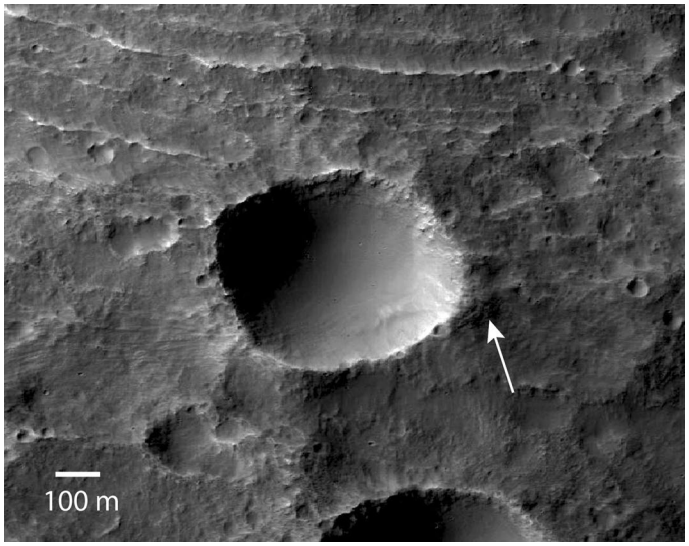

Extended Data Fig. 6 | Steeply dipping layers within a antiformal fold complex. A HiRISE image of the northern flank of the antiform discussed in the text reveals vertical layering (that is steeply dipping). Because the map trace of the layer oucrops are not deflected by topographic changes around and within the crater, the layers must be steeply dipping.